Changes in the SSRT Plasticity Parameters of Low-Carbon Steel with Polarization Potential in Carbonate-Bicarbonate Solution

Sviatoslav Hirnyj [1,a] and Michael J. McNallan [2,b]

[1] University of Illinois at Chicago, M/C-246, 842 W. Taylor St., Chicago, Illinois, U.S.A., currently at Karpenko Physical-Mechanical Institute, 5 Naukova St., Lviv, Ukraine

[2] University of Illinois at Chicago, M/C-246, 842 W. Taylor St., Chicago, Illinois, U.S.A.

[a] hirnyj@ipm.lviv.ua, [b] mcnallan@uic.edu

Keywords: plasticity parameters, slow-strain rate technique, low-carbon steel, stress corrosion cracking, electrochemical potential, hydrogen.

Abstract. This paper reports on the influence of the electrochemical polarization potential on ductility at fracture of 1020 steel immersed in carbonate-bicarbonate solution at 52 °C during slow-strain rate testing (SSRT) under straining rate $10^{-6}\,s^{-1}$. All the plasticity parameters showed the same dependency on the applied potential, but reduction of area exhibited the highest sensitivity and smallest scatter. Area reduction ψ remains almost unchanged (~53%) at potentials above −600...−550 mV (on the standard hydrogen scale), while at lower potentials the apparent ductility of steel decreases to ψ (−1030 mV) = 24 %. The changes in area reduction at increasing cathodic potentials was attributed to the role of hydrogen, though the presented data could not explain why the embrittling effect of hydrogen is manifested even at potentials anodic to free corrosion potential, where transgranular SCC is observed. The insensitivity of plasticity parameters to the ranges of potential where a network of intergranular stress corrosion cracks is formed brings attention to the usefulness of these parameters for characterization of SCC.

Introduction

The SCC studies performed during the past few decades have exposed a wide spectrum of metal-environment systems that exhibit crack initiation and propagation under specific combinations of surface conditions and mechanical straining, while without the surrounding environment and specific surface conditions no failure of the material could be detected [1,2]. SCC phenomena are rooted in a synergistic effect of the influence of mechanical and chemical fields on the material [3], so it would be incorrect to consider only only one of a fracture-mechanical or chemical approach to the problem. These two are quite different, however, mostly from the scale point of view, since chemistry operates with interatomic interactions and electron structure of matter, while fracture mechanics looks at the material as a continuum, usually with homogeneous properties. Continuum mechanics could not possibly explain phenomena at the atomistic or even electronic level since this is where there is no more continuity and all the formalism has to collapse.

A chemical approach to SCC, at first sight, seems to be in a superior position since it can incorporate mechanical properties through the interatomic bonding energy, which together with crystallographic parameters defines the strength of the material. This chemical approach to the materials strength is indeed very good, but only for the materials of highest purity, preferably in a monocrystalline condition. Such materials, however, are usually not susceptible to SCC. Moreover, they exist only in small quantities and are used for special applications where SCC is not an issue of concern. Real structural materials, which do exhibit SCC failures, could easily contain half of the periodic table of elements and huge number of 0D-, 1D-, 2D- and 3D-defects/imperfections with several different phases dispersed in a polycrystalline material. Such compositions render rigorous chemical analysis of mechanical behavior practically impossible.

Since the explanation of SCC phenomenon is somewhere in between the two approaches, there is no possibility for advancing, except to move in the direction of severely increasing the number of variables in the chemical description of the process, or to move towards finite element analysis of the system, substituting atoms for nodes in the grid that simulates atomic arrangement in real material. Both of these approaches, eventually, should meet in a chemomechanical model of the material. The number of studies in chemomechanics / mechanochemistry with application of computational facilities is growing quickly and the time is probably near when SCC will be modeled and analyzed by use of super computers. Until then, however, we are destined to labor in the labs and exercise our knowledge and fantasy in every attempt to bridge the gap between these two approaches. We have to do it in order to accumulate sufficient databanks of relative information and to generate enough plausible ideas, hypotheses and theories concerning the origins of SCC.

Returning from the dreams about the future to the contemporary realities, let us look at some results related to the area of carbonate SCC of low-carbon and low-alloy steels – a type of SCC discovered half a century ago on high pressure transmission pipelines. A descriptive term *carbonate* is used here to emphasize a specific role of a certain chemical species – carbonate ions – and, thus, to place this type of SCC into a class with *sulfide SCC* and *caustic SCC* – other distinct types of SCC where the role of chemical species defines the process of crack initiation and propagation. Although numerous studies have been dedicated to this type of failure so far [4-6] with much parameterization of both mechanical and chemical constants and variables there is still much need for data, with the hope that future analyses will provide a comprehensive explanation for this type of failure.

We studied SCC of low-carbon steel immersed into an electrolyte containing a concentrated solution of carbonate and bicarbonate (a.k.a. hydrocarbonate) anions, the former being well known from beverages and the latter from baking soda, both easily found in many households. It has been discovered that such an electrolyte could be formed between the disbonded coating and the metal surface of buried transmission pipelines under the influence of cathodic protection. The presence of such an electrolyte and tensile stress in the upper elastic range can cause SCC of most carbon and low-alloyed steels with one additional requirement: the electrochemical potential of the surface has to be in the narrow range of potentials responsible for the formation of specific films with certain mechanical properties and chemical compositions [6].

Among the key factors that define the mechanism of stress-corrosion damage is the electrochemical potential – a thermodynamic parameter that together with temperature and the activities of chemical species defines the electrochemical equilibria and the most stable (under the circumstance) chemical compounds on a metal surface [6,7]. Among the other effects, the electrochemical potential can intensify the effect of hydrogen, or stimulate the localized anodic dissolution in the crack tip (a chemical mechanism for crack advancement). We are not going to elaborate here on the electrochemical mechanisms of the formation of surface films, or other electrochemical processes, but to show how a purely chemical parameter, which is a surface electrochemical potential, can affect the otherwise identical combination of material-environment-stress conditions, reflected by the changes in the plasticity parameters of the failed specimens. For those who approach SCC from the fracture mechanics view point, this work might serve as an illustration not only of the importance of chemical parameters in such types of failures, but also of the validity of utilization of the plasticity parameters in evaluation of SCC damage.

Experimental Approach

Material. We studied cylindrical samples machined from cold-drawn rods 7.9 mm in diameter made of a typical low carbon steel AISI type 1020 with the following chemical composition of the most important components: C – 0.17%, Mn – 0.77%, Si – 0.016%, P+S – 0.03%. This material consisted mainly of two phases – ferrite (α-Fe) and pearlite (a mixture of α-Fe and iron carbide Fe_3C). Microstructural analysis of a transverse section of the sample, conducted with the help of

Leco 300 Metallograph revealed a lamellar morphology of pearlite illustrated on Fig. 1 (pearlite is a darker phase) with the ASTM grain size number 11. The measured hardness of the material was HRB 90.5-92.5, suggesting percent of cold work of about 50 %.

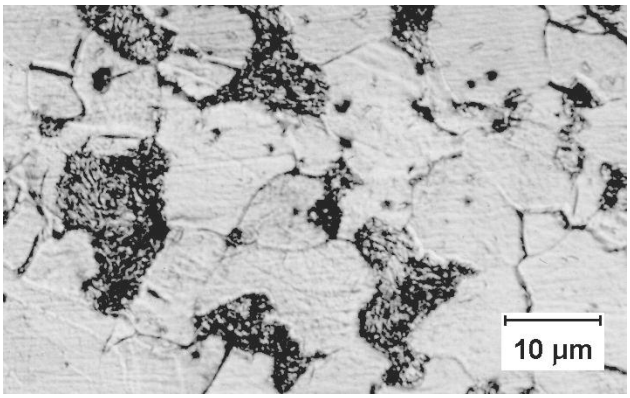

Fig. 1. Transverse section of the cold-drawn rod made of 1020 steel.

Slow-strain rate technique (SSRT). SSRT together with optical microscopy was used to provide information on a synergistic effect of mechanical and chemical forces on the material. SSRT has proven to be a useful and probably the most effective laboratory method for studying SCC, allowing one to accumulate stress-corrosion data in a relatively short period of time [8]. This is very important in studies of SCC since this type of failure is often associated with very long incubation times required for crack initiation, a fact that is especially relevant to carbonate SCC of pipeline steels, where crack initiation time could be as long as decades. Parkins and coworkers have proven that the application of SSRT in studying carbonate SCC can quickly give valuable information needed for parameterization of this type of failure [9-11].

Similarly to a conventional tensile tester, SSRT employs dynamic straining of the specimen monotonically increasing strain to failure, however, with considerably slower straining rates [12]. The SCC data produced by this method is very dependent on the strain rate. If the specimen is strained too quickly, SCC is not manifested because the rate of stress-enhanced electrochemical reactions involved in the crack growth is not sufficient and metal fails in a ductile manner, as if there is no effect of surrounding environment. On the other hand, if the straining is too slow, the kinetics of the passive film growth are high enough to sustain the crack tip under a stable passive condition, which is not influenced by strain sufficiently to fracture the passive film and produce any crack growth [8]. As reported by Parkins and Zhou [11] a $2 \cdot 10^{-6}$ s^{-1} strain rate is able to generate SCC in carbon steel in carbonate-bicarbonate solutions of different compositions and temperatures. Based on this information, we constructed an SSRT machine that was able to generate strain rates from $0.7 \cdot 10^{-6}$ s^{-1} and greater in samples having 50 mm gage length. The results reported here are related only to the set of the SSRT experiments obtained at the lowest strain rate of about $0.8 \cdot 10^{-6}$ s^{-1}. This strain rate was shown to support propagation of stress-corrosion cracks and provide experimental results in a reasonably short time for testing of a single specimen (about 20-30 hours depending on surface conditions).

The load applied to the sample was measured with the help of StrainSert-5000 load cell and strain gage conditioner, while the rate of straining of the sample was calculated from the readings of a tachometer.

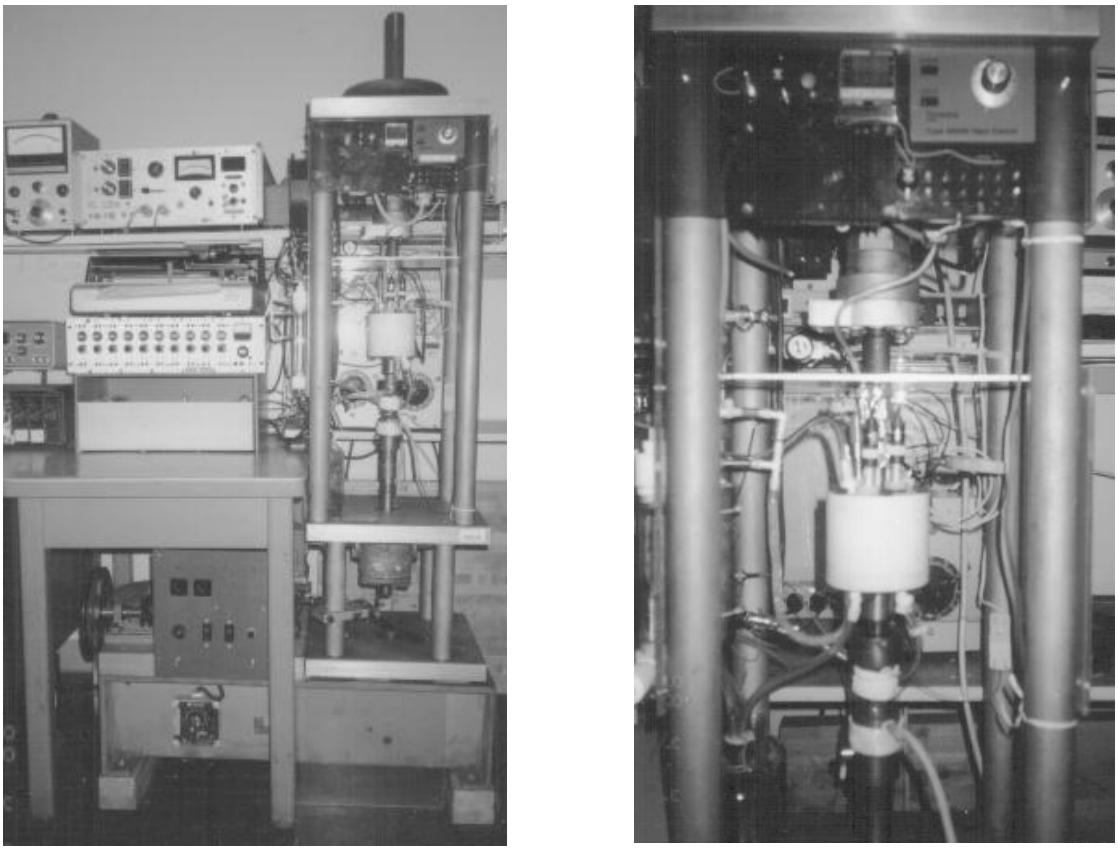

a b

Fig. 2. Slow-strain rate tensile machine with electronic equipment for electrochemical potential control of the metal surface (a) and closer look at the electrochemical cell, load cell and temperature controlling module (b).

Corrosive environment. A concentrated carbonate-bicarbonate solution that contains 1N $NaHCO_3$ and 1N Na_2CO_3 has long been adopted as a standard corrosive solution for screening the materials regarding their SCC susceptibility, though numerous studies were conducted on other mixtures of carbonate and bicarbonate salts in relation to SCC of pipeline steels and they are mostly reported by Parkins and coworkers [13]. In our study, only this standard solution made from reagent grade chemicals and deionized water was used. The chamber containing the solution was made of Teflon (PTFE) and was equipped with a deaeration system; temperature control, which provided stability of temperature to ±0.3 K; and electrodes for measuring the electrochemical potential of the surface and for providing current needed to keep that potential constant with the help of potentiostat.

Electrochemical polarization potential. Electrochemical control of the samples was provided either by EG&G 173 PARC or by Model 410 Electrosynthesis potentiostat with polarization current recorded throughout the duration of the experiment. The samples were polarized potentiostatically, i.e. at constant potentials ranging from −1030 mV to −230 mV (all potentials are presented relative to standard hydrogen electrode scale). This range covered electrochemical potentials from vigorous hydrogen evolution (needed for cathodic hydrogen absorption by metal) to highly stable passivity, where the metal surface was covered with oxide-hydroxide film.

Temperature. In studies of carbonate SCC, one of the important parameters is temperature. It was reported by Parkins that increasing the temperature of the carbonate-bicarbonate solution from ambient to 80 °C causes the stress-corrosion crack velocity to increase by one order of magnitude [6,11]. For our studies, we selected an intermediate temperature 52 °C (325 K – a convenient value for thermodynamic calculations) instead of either low (20-25 °C) or high temperature (70-80 °C) for several reasons. Firstly, the SCC data for this temperature range is rather scarce, though intermediate temperatures are very plausible for the pipeline steels that experience carbonate SCC failures. Secondly, this temperature provides sufficiently high kinetic parameters of the processes – crack growth rate, corrosion film growth rate, diffusion coefficient. Also, 52 °C guarantees good thermal stability of the labware – electrochemical electrodes, PTFE chambers, sealings, temperature controllers, load cell.

Testing procedure. Right before being placed into the testing chamber, each SSRT sample with a gage length of 50 mm and diameter of 5 mm was wet polished with #320 and #400 emery paper and degreased with acetone. Before the desired polarization was imposed upon the interface separating metal and environment, a cathodic pretreatment at −1030 mV was applied for 1 minute. This treatment was applied immediately after the chamber was filled with solution, but before it reached the desired temperature. When temperature reached 52 °C, the straining of the sample was activated.

After the sample was fractured, the cell was quickly disassembled, two specimen pieces were quickly rinsed with deionized water, air-jet dried and instantly brought for Raman spectral analysis in order to establish the chemistry of the surface films. Subsequently, visual examination was performed, ductility parameters measured, and, finally, the parts of samples were delivered for metallographic examination of their cross sections. From the list of inspection techniques only microhardness revealed no insights into the failure mechanism. Among the plasticity parameters, we calculated relative elongation δ, relative reduction of area ψ, and the ratio between the maximum (ultimate) load sustained by the sample during straining P_{max} and load at failure P_f. Correlations between the ductility parameters and electrochemical potential were sought.

Results

Visual and metallographic examination. Metallographic and visual inspection revealed several distinct appearances which could be correlated with the tested electrochemical potentials and the corresponding stress corrosion (chemomechanical) damage. In the majority of samples containing stress corrosion cracks the cracks were secondary cracks located mostly in the necked region of the sample, *i. e.* in the areas of high plastic deformation. For the samples covered with visible corrosion products, the number of secondary cracks was very high. At certain potentials, cracks were spaced only 10…20 μm apart, thus approaching the average grain size (Fig. 1). This confirmed that grain boundaries of the material emerging to the metal surface become initiation sites for stress corrosion cracks. Based on these observations, four distinct ranges of electrochemical potential with different surface appearances and failure modes could be established:

1. below free corrosion potential E_{cor} = −655 mV: brittle failure, no corrosion film;
2. from E_{cor} to −440 mV: transgranular cracking, matte greenish-grayish corrosion products;
3. from −430 mV to −320 mV: intergranular cracking, glossy dark-grey-to-black corrosion scale; and
4. above −320 mV: no corrosion cracking, ductile rupture, no visible corrosion products.

Thus, the electrochemical potential is among the key parameters defining both the corrosion activity of metal and its mode of rupture.

Plasticity parameters. All three parameters which were employed for evaluation of the plasticity change during SSRT, δ, ψ, and ratio P_{max}/P_f responded to the applied electrochemical potential, with their dependencies being quite similar. Of these three, however, the relative reduction of area ψ exhibited the highest sensitivity and the smallest scatter. Therefore, we will present only

dependency $\psi(E)$. Fig. 3 depicts this data together with ranges of potentials responsible for different chemomechanical types of damage.

From Fig. 3 we can separate the samples into two categories: those tested at potentials below –600...–500 mV and those above. The former exhibited a noticeable tendency for gradual reduction of plasticity with increase of cathodic (negative) potential, while the latter seem insensitive to the applied potential. The average value of ψ for the second group is ~53 %, which well agrees with the ψ value obtained for the samples ruptured in air or in glycerin-alcohol mixture, i.e. under non-aggressive environments. For stronger cathodic potentials reduction of area decreases through $\psi(-630\text{ mV}) = 44\ \%$ down to $\psi(-1030\text{ mV}) = 24\ \%$, which is more than twofold compare to $\psi = 53\ \%$.

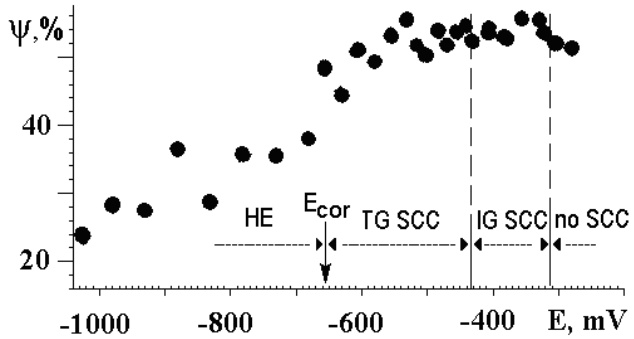

Fig. 3. The effect of electrochemical polarization potential on reduction of area at fracture of SSRT samples tested in 1N $NaHCO_3$ + 1N Na_2CO_3 solution at 52 °C. HE – hydrogen embrittlement, E_{cor} – open circuit electrochemical potential, a.k.a. *corrosion* potential, TG SCC – transgranular SCC, IG SCC – inetrgranular SCC.

Discussion

A conclusion from the $\psi(E)$ dependency is that the embrittling role of hydrogen increases with cathodic (negative) potentials. Closer examination of the dependency of $\psi(E)$ as depicted by Fig. 3, shows that the ductility parameter is completely insensitive to intergranular SCC. In the transgranular SCC range, it shows some decrease with cathodic potentials. This change, however, is not a result of a developed network of cracks since this would also be reflected for the intergranularly cracked samples. Most probably, it is a result of absorbed hydrogen, whose embrittling tendency begins at potentials –550...–600 mV, anodic to the free corrosion potential at –655 mV [14], but apparently above the reversible potential for hydrogen evolution [15].

Despite the huge bibliography dedicated to hydrogen related fractures, there is still much to be done to clarify the different scenarios that hydrogen has on metals, especially, iron-based materials. During such failures the microstructure of metal could be irreversibly destroyed due to the formation of voids filled with high-pressure molecular hydrogen or methane [16,17]. Our discussion is concerned with significantly lower hydrogen activities (often measured in fractions of ppm), insufficient for microstructural damage, but definitely important in facilitating material's fracture when other factors, like aggressive media and applied stress, are present. In this case, the term hydrogen embrittlement is often used. This term obviously emphasizes the loss of ductility of the material, as evaluated with plasticity parameters.

Among the existing theories of hydrogen-related damage under lower hydrogen activity only two, namely hydrogen-enhanced local plasticity and hydrogen-enhanced decohesion, have proven

convincing for non-hydride forming H–Me systems. The theory of hydrogen-enhanced local plasticity – HELP – was introduced by Birnbaum (who has to be credited for enormous TEM work that focused on the evidences for hydrogen action in metals) [18] while the theory of hydrogen-enhanced decohesion could be ascribed to Oriani [19,20], with both theories having had their predecessors who paved the way [21-23]. The most intriguing name has the HELP theory since it discloses the scale dependency of the terms *brittle* and *ductile/plastic*. On the macro-scale, hydrogen-induced damage looks brittle and exhibits a decrease of the plasticity parameters, while on a sub-microscale the mechanism of fracture has been revealed as related to increased mobility of dislocations rather than cleavage – the attributes of a ductile fracture not a brittle one [18].
Metallographic examination of the severity of stress corrosion crack growth disclosed that IG cracks are deeper than TG, with both modes exhibiting the deepest damage at potentials near the TG-IG transition, i.e. –400...–450 mV. This means (based on Fig. 3) that the formation of a network of secondary stress corrosion cracks on the surface during dynamic straining could not influence the integral parameter of area reduction at fracture. Definitely, the average depths of these secondary cracks were insufficient to influence ψ and this could be explained with short duration of the time window when the level of stress and the kinetics of corrosion processes were such that supported stress corrosion crack growth. On the other hand, ψ was very sensitive to hydrogen embrittlement reflecting interaction between the absorbed hydrogen and dislocations.
Since the plasticity parameters do not reflect the development of stress corrosion cracks during SSRT, the question regarding the role of hydrogen during intergranular or transgranular modes of failure has to be answered using different evidence, which goes beyond the scope of this paper. Basically, in case of SCC, especially in actively corroding systems (as in our case), the picture is very complicated due to the chemical and electrochemical interactions and transport of matter to and from the surface, including the walls of growing cracks and the crack tips. In this process, besides the mechanical and possible hydrogen-related mechanisms, there is also an electrochemical mechanism that leads to dissolution of metal at the crack tip, with corrosion films playing important roles. We have to note here, that the major difficulty in tracing the role of hydrogen experimentally is its extremely low solubility and high diffusivity in iron at ambient temperatures, and its light weight that makes its quantitative evaluation in metal a complicated problem.

Conclusions

The effect of electrochemical potential on ductility at fracture of 1020 steel immersed in carbonate-bicarbonate solution at 52 °C during slow-strain rate testing under straining rate $10^{-6}\,s^{-1}$ was studied. All the plasticity parameters showed the same dependency on the applied potential, but reduction of area exhibited the highest sensitivity and smallest scatter. Area reduction ψ remained almost unchanged (~53%) at potentials above −600...−550 mV, while at lower potentials the apparent ductility of steel decreases to ψ (−1030 mV) = 24 %. The decay of plasticity was attributed to the role of hydrogen, though the presented data could not explain why the embrittling effect of hydrogen is manifested even at potentials anodic to free corrosion potential, where transgranular SCC is observed. The insensitivity of plasticity parameters to the ranges of potential where a network of intergranular stress corrosion cracks is formed brings attention to the usefulness of these parameters for characterization of SCC.

Literature cited

[1] R.C. Newman, in: *Corrosion Mechanisms in Theory and Practice*, edited by P. Marcus and J. Oudar, Marcel Dekker (1995), p. 311.

[2] Environmentally induced cracking, in: *Corrosion in Petrochemical Industry*, edited by L. Garverick, ASM Intern.: Materials Park, OH, USA (1994), p. 39.

[3] R.H. Jones, in: *ASM Metals Handbook "Corrosion"*, Vol. 13, 9th ed., ASM Intern.: Materials Park, OH (1987), p. 145.

[4] B.N. Leis and W.J. Walsh, in: *Environmentally Assisted Cracking*. *Science and Engineering*, edited by W.B. Lisagor, T.W. Crooker and B.N. Leis, ASTM: Philadelphia, ASTM STP 1049 (1990), p. 243.
[5] B.N. Leis: *Recurrent SCC in gas-transmission pipelines: service history and material property considerations*, Battelle, NG-18 report No.210, 1994.
[6] R.N. Parkins: *Overview of intergranular SCC research activities*, University of Newcastle upon Tyne, PR-232-9401, 1994.
[7] M. Pourbaix: Corr. Sci. Vol. 30 (1990), p. 963.
[8] R.N. Parkins, in: *SSRT for the Evaluation of Environmentally Induced Cracking. Research and Engineering Application",* edited by R.D. Kane, ASTM: Philadelphia, STP 1210 (1993), p. 7.
[9] R.N. Parkins: Corrosion Vol. 43 (1987), p. 130.
[10] R.N. Parkins, E. Belhimer and W.K. Blanchard: Corrosion Vol. 49 (1993), p. 951.
[11] R.N. Parkins and S. Zhou: Corr. Sci. Vol. 39 (1997), p. 159.
[12] ASTM G-129 Standard practice for slow strain rate testing to evaluate the susceptibility of metallic materials to environmentally assisted cracking, DOI: 10.1520/G0129-00R06, ASTM International, West Conshohocken, PA,. www.astm.org.
[13] R.N. Parkins, C.S. O`Dell and R.R. Fessler: Corr. Sci. Vol. 24 (1984), p. 343.
[14] S.I. Hirnyj: Mater. Sci. Vol. 37 (2001), p. 491.
[15] M. Pourbaix: *Atlas of Electrochemical Equilibria in Aqueous Solutions*, Oxford: Pergamon Press, 1966.
[16] S.P. Lynch: J. Mater. Sci. Vol. 20 (1985), p. 3329.
[17] D.P. Williams and H.G. Nelson: Metall. Trans. Vol. 1 (1970), p. 63.
[18] H.K. Birnbaum, in: *Hydrogen Effects on Materials Behavior*; edited by N.R. Moody and A.W. Thompson, TMS (1990), p. 639.
[19] R.A. Oriani: Berichte der Bunsen-Gesellschaft fuer Phys. Chemie Vol. 76 (1972), p. 848.
[20] R.A. Oriani and P.H. Josephic: Acta Metall. Vol. 25 (1977), p. 979.
[21] N.J. Petch and P. Stables: Nature Vol. 169 (1952), p. 842.
[22] A.R. Troiano: Trans. ASM Vol. 52 (1960), p. 54.
[23] C.D. Beachem: Metall. Trans. Vol. 3 (1972), p. 437.